

# Cohesive property of magnetized neutron star surfaces: Computations and implications

Z. Medin<sup>a</sup>, D. Lai<sup>a</sup>

<sup>a</sup>*Center for Radiophysics and Space Research, Department of Astronomy, Cornell University, Ithaca, NY 14853*

---

## Abstract

The cohesive energy of condensed matter in strong magnetic fields is a fundamental quantity characterizing magnetized neutron star surfaces. The cohesive energy refers to the energy required to pull an atom out of the bulk condensed matter at zero pressure. Theoretical models of pulsar and magnetar magnetospheres depend on the cohesive properties of the surface matter in strong magnetic fields. For example, depending on the cohesive energy of the surface matter, an acceleration zone (“polar gap”) above the polar cap of a pulsar may or may not form. Also, condensation of the neutron star surface, if it occurs, can significantly affect thermal emission from isolated neutron stars. We describe our calculations of the cohesive property of matter in strong magnetic fields, and discuss the implications of our results to the recent observations of neutron star surface emission as well as to the detection/non-detection of radio emission from magnetars.

*Key words:* stars: pulsars, stars: neutron, stars: magnetic fields, radiation mechanisms: non-thermal

---

## 1 Introduction

Recent observations of neutron stars have provided a wealth of information on these objects, but they have also raised many new questions. For example, with the advent of x-ray telescopes such as Chandra and XMM-Newton, detailed observations of the thermal radiation from the neutron star surface have become possible. These observations show that some nearby isolated neutron stars (e.g., RX J1856.5-3754) appear to have featureless, nearly blackbody spectra (Burwitz et al. 2003; van Kerkwijk & Kaplan 2006). Radiation from a bare condensed surface (where the overlying atmosphere has negligible optical depth) has been invoked to explain this nearly perfect blackbody emission (e.g., Burwitz et al. 2003; Mori & Ruderman 2003; van Adelsberg et al. 2005;

Turolla et al. 2004; Perez-Azorin et al. 2006). However, whether surface condensation actually occurs depends on the cohesive properties of the surface matter.

Equally puzzling are the observations of the recently-discovered anomalous x-ray pulsars (AXPs) and soft gamma-ray repeaters (SGRs) (see Woods & Thompson 2005 for a review). Though these stars are believed to be magnetars, neutron stars with extremely strong magnetic fields ( $B \geq 10^{14}$  G), they mostly show no pulsed radio emission (but see Camilo et al. 2006) and their x-ray radiation is too strong to be powered by rotational energy loss. By contrast, several high-B radio pulsars with inferred surface field strengths similar to those of magnetars have been discovered (e.g., Kaspi & McLaughlin 2005). A deeper understanding of the distinction between pulsars and magnetars requires further investigation of the mechanisms by which pulsars and magnetars radiate and of their magnetospheres where this emission originates. Theoretical models of pulsar and magnetar magnetospheres depend on the cohesive properties of the surface matter in strong magnetic fields (e.g., Ruderman & Sutherland 1975; Arons & Scharlemann 1979; Usov & Melrose 1996; Harding & Muslimov 1998; Gil et al. 2003; Beloborodov & Thompson 2006). For example, depending on how strongly bound the surface matter is, an acceleration zone (“polar gap”) above the polar cap of a pulsar may or may not form, and this will affect pulsar radio emission and other high-energy emission processes.

The cohesive property of the neutron star surface matter plays a key role in these and many other neutron star processes and observed phenomena. The cohesive energy refers to the energy required to pull an atom out of the bulk condensed matter at zero pressure. For magnetized neutron star surfaces this cohesive energy can be many times the corresponding terrestrial value, due to the strong magnetic fields threading the matter.

In two recent papers (Medin & Lai 2006a,b, hereafter ML06a,b), we calculated the cohesive energy for H, He, C, and Fe surfaces at field strengths between  $B = 10^{12}$  G to  $2 \times 10^{15}$  G. We now wish to investigate some implications of these calculations. This paper is organized as follows. In §II we briefly summarize the cohesive energy results of ML06 used in this paper. In §III we discuss the possible formation of a bare neutron star surface. The conditions for the formation of a polar vacuum gap in pulsars and magnetars are presented in §IV. We summarize our results in §V. A more detailed/comprehensive study of these and related issues will be presented in a future paper (Medin & Lai 2007, in preparation).

## 2 Numerical Calculations of Condensed Matter in Strong Magnetic Fields

It is well-known that the properties of matter can be drastically modified by strong magnetic fields. The natural atomic unit for the magnetic field strength,  $B_0$ , is set by equating the electron cyclotron energy  $\hbar\omega_{Be} = \hbar(eB/m_e c) = 11.577 B_{12}$  keV, where  $B_{12} = B/(10^{12}$  G), to the characteristic atomic energy  $e^2/a_0 = 2 \times 13.6$  eV (where  $a_0$  is the Bohr radius):

$$B_0 = \frac{m_e^2 e^3 c}{\hbar^3} = 2.3505 \times 10^9 \text{ G.} \quad (1)$$

For  $b = B/B_0 \gtrsim 1$ , the usual perturbative treatment of the magnetic effects on matter (e.g., Zeeman splitting of atomic energy levels) does not apply. Instead, the Coulomb forces act as a perturbation to the magnetic forces, and the electrons in an atom settle into the ground Landau level. Because of the extreme confinement of the electrons in the transverse direction (perpendicular to the field), the Coulomb force becomes much more effective in binding the electrons along the magnetic field direction. The atom attains a cylindrical structure. Moreover, it is possible for these elongated atoms to form molecular chains by covalent bonding along the field direction. Interactions between the linear chains can then lead to the formation of three-dimensional condensed matter (Ruderman 1974; Ruder et al. 1994; Lai 2001).

Previous calculations of the cohesive energy of one-dimensional chains and condensed matter were done by Jones (1985, 1986) and Neuhauser et al. (1987). These earlier calculations adopted some crude approximations (e.g., band structure was not properly treated by Neuhauser et al.) and gave somewhat conflicting results. These calculations were also restricted to moderate neutron star field strengths ( $B = 10^{12}$ - $10^{13}$  G).

Our new calculations (ML06a,b) are based on density functional theory. ML06a summarizes our calculations for various atoms and molecules in magnetic fields ranging from  $10^{12}$  G to  $2 \times 10^{15}$  G for H, He, C, and Fe, representative of the most likely neutron star surface compositions. Numerical results of the ground-state energies are given for  $\text{H}_N$  (up to  $N = 10$ ),  $\text{He}_N$  (up to  $N = 8$ ),  $\text{C}_N$  (up to  $N = 5$ ), and  $\text{Fe}_N$  (up to  $N = 3$ ), as well as for various ionized atoms. ML06b summarizes our calculations for infinite chains for H, He, C, and Fe in that same magnetic field range. For relatively low field strengths, chain-chain interactions play an important role in the cohesion of three-dimensional (3D) condensed matter; an approximate calculation of 3D condensed matter is also presented in ML06b. Numerical results of the ground-state and cohesive energies, as well as the electron work function and the zero-pressure condensed matter density, are given for  $\text{H}_\infty$  and H(3D),  $\text{He}_N$  and He(3D),  $\text{C}_\infty$  and C(3D),

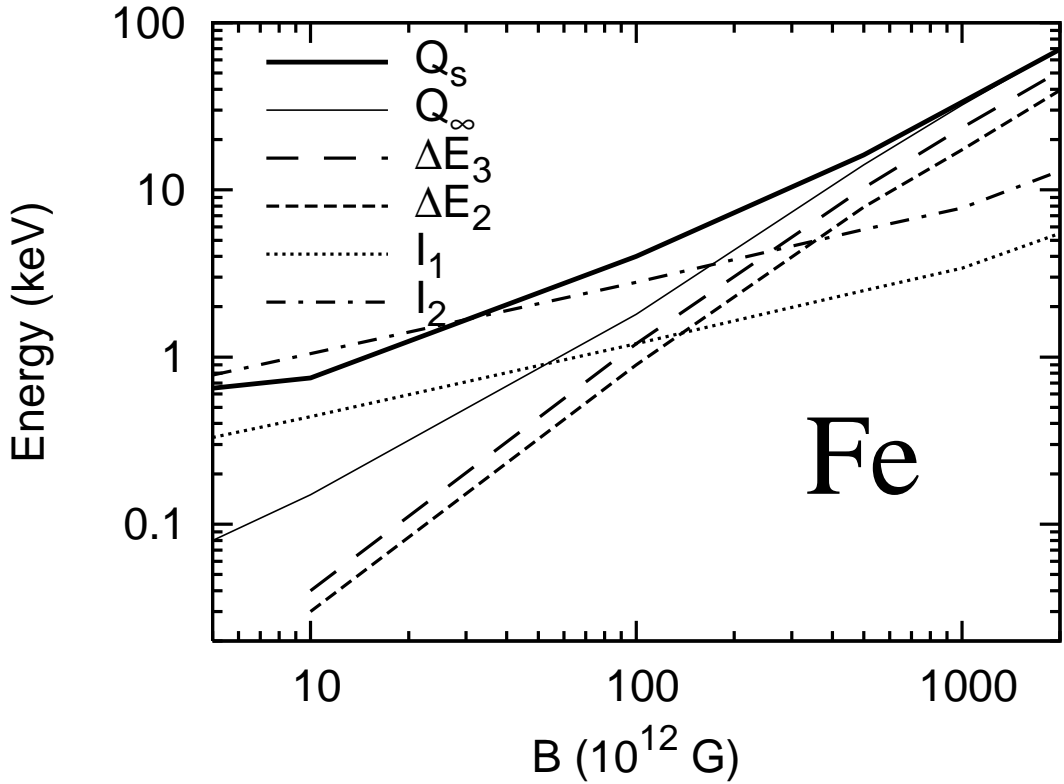


Fig. 1. Cohesive energy  $Q_s$  and molecular energy difference  $\Delta E_N$  for iron (where  $\Delta E_N = E_N/N - E_1$ ) as a function of the magnetic field strength. The symbol  $Q_\infty$  represents the cohesive energy of one-dimensional chains, and  $I_1$  and  $I_2$  are the first and second ionization energies of the Fe atom.

and  $\text{Fe}_\infty$  and  $\text{Fe}(3\text{D})$ .

Some numerical results from ML06a,b are provided in graphical form in Figs. 1 and 2. Figure 1 shows the cohesive energies and molecular energy differences  $\Delta E_N = E_N/N - E_1$  for Fe, where  $E_1$  is the atomic ground-state energy and  $E_N$  is the ground-state energy of the  $\text{Fe}_N$  molecule. Fig. 2 shows the electron work functions for He, C, and Fe, as a function of field strength.

### 3 Condensation of Neutron Star Surfaces in Strong Magnetic Fields

As seen from Fig. 1, the cohesive energies of condensed matter increase with magnetic field. We therefore expect that for sufficiently strong magnetic fields, there exists a critical temperature  $T_{\text{crit}}$  below which a first-order phase transition occurs between the condensate and the gaseous vapor. This has been investigated in detail for hydrogen surfaces (see Lai & Salpeter 1997), but not for other surface compositions. Here we discuss the critical temperature values for the phase transitions of Fe surfaces.

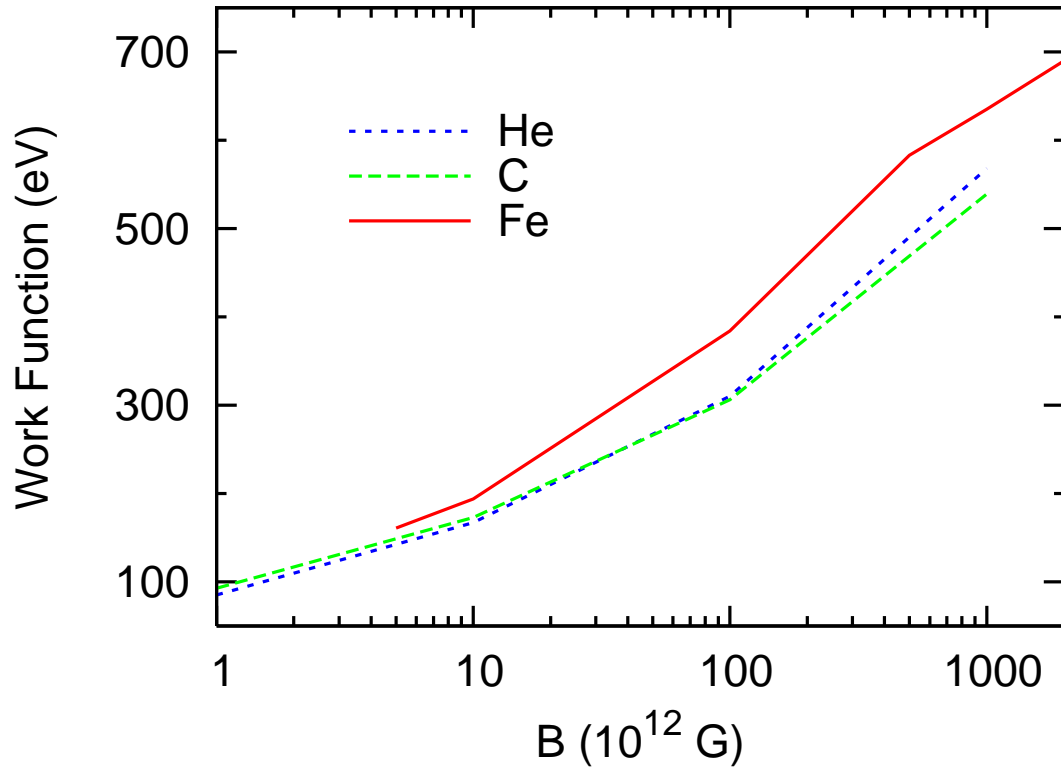


Fig. 2. The work function as a function of  $B$ , for H, He, C, and Fe infinite chains.

A precise calculation of  $T_{\text{crit}}$  is difficult to obtain at present. We can get an estimate by considering the equilibrium between the condensed phase (labeled “s”) and the gaseous phase (labeled “g”) in the ultrahigh field regime (where phase separation exists). The gaseous phase consists of a mixture of free electrons and bound ions, atoms, and molecules. For a given temperature, phase equilibrium occurs when the total pressure of the gas equals that of the condensate, and when each species in the gas is in chemical equilibrium with the condensate. To simplify the calculation we have assumed that the vapor pressure is sufficiently small so that the deviation from the zero-pressure state of the condensate is small; this is justified when the saturation vapor pressure  $P_{\text{sat}}$  is much less than the critical pressure  $P_{\text{crit}}$  for phase separation, or when  $T \ll T_{\text{crit}}$ .

We have calculated the equilibrium densities of the various species in the gaseous vapor, as a function of temperature. Some results are shown in Fig. 3, for magnetic field strengths of  $B = 10^{13}$  and  $5 \times 10^{14}$  G. The critical temperature  $T_{\text{crit}}$ , below which phase separation between the condensate and the gaseous vapor occurs, is determined by the condition  $\rho_s \simeq \rho_g$ . Using the values for  $E_N/N$  (the energy per atom in the  $\text{Fe}_N$  molecule),  $E_s$  (the ground-state energy of the condensed Fe), and  $E_{n+}$  (the energy of the  $\text{Fe}^{n+}$  ion) presented in ML06, we find  $T_{\text{crit}} \simeq 6 \times 10^5$ ,  $7 \times 10^5$ ,  $3 \times 10^6$ ,  $10^7$ , and  $2 \times 10^7$  K for

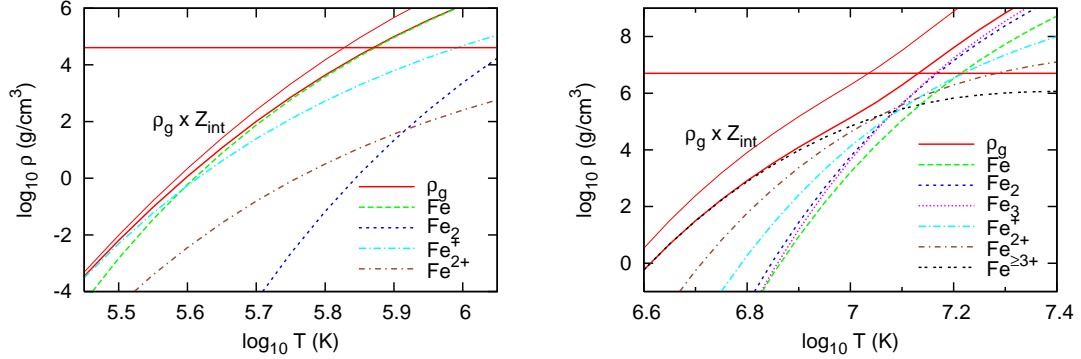


Fig. 3. The densities of various species and the total gas density in the saturated vapor of a condensed Fe surface, as a function of temperature, for  $B_{12} = 10$  (left panel) and  $500$  (right panel). The horizontal lines give the condensed matter density  $\rho_s$ . The curves labeled by “ $\rho_g \times Z_{\text{int}}$ ” give the vapor density when the internal partition functions of the atoms and molecules are included, while the other curves do not include the internal partition functions. The critical temperature is set by  $\rho_g \approx \rho_s$ .

$B_{12} = 5, 10, 100, 500$ , and  $1000$ . In terms of the cohesive energy, we have

$$kT_{\text{crit}} \sim 0.08 Q_s. \quad (2)$$

Note that although our results for the vapor densities were derived using  $\rho_g \ll \rho_s$ , while the condition for phase separation requires  $\rho_g \simeq \rho_s$ , we may still use the results to obtain an estimate of  $T_{\text{crit}}$ . The vapor density drops very rapidly with decreasing temperature, such that when the temperature is below  $T_{\text{crit}}/2$  (for example) this density is much less than the condensation density and phase transition is unavoidable. When the temperature drops below a fraction of  $T_{\text{crit}}$ , the vapor density becomes so low that the optical depth of the vapor is negligible and the outermost layer of the neutron star then consists of condensed iron. The radiative properties of such condensed phase surfaces have been studied using a simplified treatment of the condensed matter (see van Adelsberg et al. 2005 and references therein).

#### 4 Vacuum Gap Accelerators of Pulsars and Magnetars

A rapidly rotating, strongly magnetized neutron star induces a strong electric field with a component along the magnetic field lines of the star. The plasma surrounding the neutron star is assumed to be an excellent conductor, such that the charged particles in the plasma move to screen this parallel component of the electric field. The particles fill the magnetosphere with a charge density

of approximately (Goldreich & Julian 1969)

$$\rho_{GJ} = -\frac{\boldsymbol{\Omega} \cdot \mathbf{B}}{2\pi c} \frac{1}{1 - \Omega_*^2 r_\perp^2/c^2}, \quad (3)$$

where  $\boldsymbol{\Omega}$  is the rotation rate of the neutron star.

Charged particles traveling outward along the open field lines in the polar cap region of the neutron star magnetosphere will escape beyond the light cylinder. To maintain the required magnetosphere charge density these particles will have to be replenished by the neutron star surface. If the surface temperature and surface cohesive strength of a neutron star are such that the required particles are tightly bound to the stellar surface, those regions of the polar cap through which the charged particles are escaping will not be replenished. A vacuum gap will form in those regions, starting at the stellar surface and moving outward at a velocity  $v \sim c$  (e.g., Ruderman & Sutherland 1975; Cheng & Ruderman 1975; Usov & Melrose 1996; Gil et al. 2003). Obviously, the existence of this vacuum gap depends on the cohesive energy and electron work function of the condensed neutron star surface.

We note that in the absence of a vacuum gap, a polar gap acceleration zone based on the space-charge-limited flow may still develop (e.g., Arons & Scharlemann 1979; Harding & Muslimov 1998).

#### 4.1 Thermal Emission/Evaporation of Charged Particles

For neutron stars with  $\boldsymbol{\Omega} \cdot \mathbf{B}_p > 0$  ( $\mathbf{B}_p$  is the magnetic field at the polar cap), electron emission is relevant. The emission rate for electrons from the condensed surface can be calculated by assuming that these electrons behave like a free electron gas in a metal. The energy barrier they must overcome is the work function of the metal. The equilibrium electron charge density (balance between electron loss to infinity and supply by the surface) above the polar cap can be written as

$$\rho_e \simeq \begin{cases} \rho_{GJ} \exp(C_e - \phi/kT), & \phi \geq C_e kT, \\ \rho_{GJ}, & \phi \leq C_e kT, \end{cases} \quad (4)$$

where  $\phi$  is the electron work function and the parameter  $C_e \sim 30$  depends on magnetic field strength and temperature. The electron work function was calculated in ML06b and is depicted in Fig. 2.

For neutron stars with  $\Omega \cdot \mathbf{B}_p < 0$ , ion emission is relevant. The emission rate for ions from the condensed surface is more complicated. Unlike the electrons, which form a relatively free-moving gas within the condensed matter, the ions are bound to their lattice sites. To escape from the surface, the ions must satisfy three conditions. First, they must be located on the surface of the lattice. Ions below the surface will encounter too much resistance in trying to move through another ion's cell. Second, they must have enough energy to escape as unbound ions. This binding energy that must be overcome will be labeled  $E_B$ . Third, they must be thermally activated. The energy in the lattice is mostly transferred by conduction, so the ions must wait until they are bumped by atoms below to gain enough energy to escape. The characteristic frequency with which that occurs is the lattice vibration frequency.

From these three requirements for the ions, we can obtain the equilibrium ion charge density above the polar cap:

$$\rho_i \simeq \begin{cases} \rho_{GJ} \exp(C_i - E_B/kT), & E_B \geq C_i kT, \\ \rho_{GJ}, & E_B \leq C_i kT, \end{cases} \quad (5)$$

where the parameter  $C_i \sim 30$  depends on magnetic field strength and temperature.

The binding energy  $E_B$  appearing in this formula is the energy required to release an ion from the surface of the condensed matter. This is equivalent to the energy required to release a neutral atom from the surface and ionize it, minus the energy gained by returning the electrons to the surface. Thus (see Tsong 1990),

$$E_B = Q_s + \sum_{i=1}^n I_i - n\phi, \quad (6)$$

where  $Q_s > 0$  is the cohesive energy,  $I_i > 0$  is the  $i$ th ionization energy of the atom (so that  $\sum_{i=1}^n I_i$  the energy required to remove  $n$  electrons from the atom),  $n > 0$  is the charge of the ion, and  $\phi > 0$  is the electron work function. All of these quantities were calculated in ML06b (see Figs. 1 and 2).

#### 4.2 Conditions for Forming a Vacuum Gap

If the ions or electrons that are required to fill the magnetosphere can do so freely, no gap will form. From Eqs. (4) and (5), we can see that no polar gap

will form if

$$\phi \lesssim C_e kT \sim 2.6T_6 \text{ keV} \quad (7)$$

for a negative polar magnetosphere ( $\Omega \cdot \mathbf{B}_p > 0$ ), and

$$E_B \lesssim C_i kT \sim 2.6T_6 \text{ keV} \quad (8)$$

for a positive polar magnetosphere ( $\Omega \cdot \mathbf{B}_p < 0$ ). Note that the two conditions are related by almost the same factor of  $kT$ . This is coincidental, as  $C_e$  and  $C_i$  depend on completely different constants and functions of  $B$  and  $T$ .

For neutron stars in general, the electron work function  $\phi$  is much less than  $30kT$  (see Fig. 2), so electrons are easily removed from the condensed surface. No gap forms for a negative polar magnetosphere under neutron star surface conditions. The ion binding energy  $E_B$ , on the other hand, is generally larger than  $30kT$ . Ions can tightly bind to the condensed surface and a polar gap can form under certain neutron star surface conditions. Figure 4 shows the critical temperature (determined by  $E_B = C_i kT$ ) below which a vacuum gap can form for the Fe, C, and He surfaces.

## 5 Discussion

Our calculations show that there are a range of neutron star magnetic field strengths and surface temperatures where the condensed surface will have an important effect on radiation from these stars. For example, if the surface composition is Fe, then strong-field neutron stars ( $B \gtrsim 10^{13}$  G) with moderate ( $T \lesssim 10^6$  K) surface temperatures should have atmospheres/vapors that are effectively transparent to thermal radiation, so that the emission becomes that from a bare condensed surface. This may explain the nearly blackbody-like radiation spectrum observed from the nearby isolated neutron star RX J1856.5-3754 (e.g. Burwitz et al. 2003; van Adelsberg et al. 2005; Ho et al. 2006).

Our work also indicates that for magnetar-like surface magnetic field strengths, a vacuum acceleration gap may form in the polar cap region of the neutron star, provided that the cap temperature is not too high. As mentioned before, recent observations (e.g., Kaspi & McLaughlin 2005) show that magnetars and radio pulsars overlap somewhat in their ranges of magnetic field strengths but most magnetars do not have pulsed radio emission. One possibility is that the magnetar also has radio emission, but the pulse is beamed away from us. On the other hand, magnetars typically have surface temperatures 3-5 times larger than those of high-B radio pulsars (see, e.g., Kaspi & Gavriil 2004

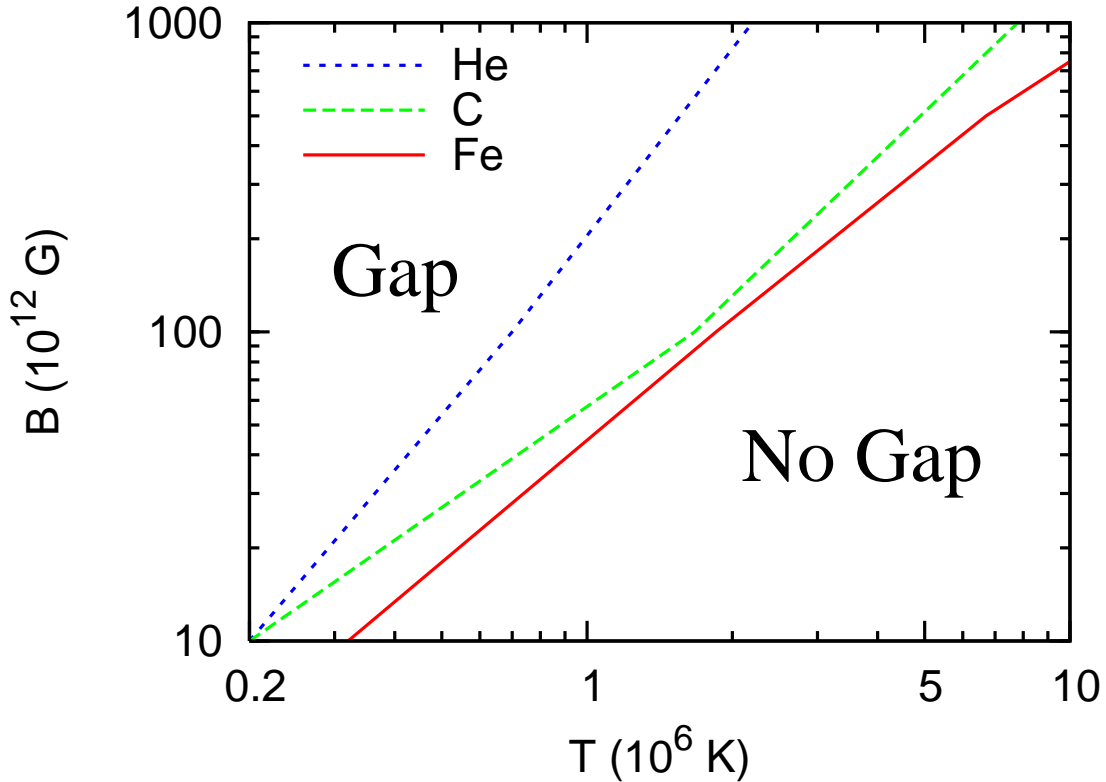


Fig. 4. The condition for the formation of a vacuum polar gap above He, C, and Fe neutron star surfaces, when the magnetosphere is positive over the poles ( $\Omega \cdot \mathbf{B}_p < 0$ ).

and Kaspi & McLaughlin 2005). We therefore speculate that a key difference between magnetars and high-B radio pulsars is their difference in the surface temperature. If the surface binding energy is such that at the low surface temperature of a radio pulsar charged particles are held tightly while at the significantly higher surface temperature of a magnetar these particles flow freely out into the magnetosphere, under the polar gap model we will have the situation where the pulsar shows pulsed radio emission and the magnetar does not (see Fig. 4). Note that the field strengths are inferred from the neutron star spin parameters, so it could be that these inferred strengths are incorrect. This would require a systematic error in the inferred field strengths of magnetars, due perhaps to the non-dipole nature of these superstrong magnetic fields.

The recent detection of the radio emission from a transient AXP (Camilo et al. 2006) is of great interest. The emission may have been triggered by a rearrangement of the surface magnetic field, which made pair cascades possible. We note that the occurrence of pair cascades depends strongly on the field line curvature in the original vacuum gap model.

## 6 Acknowledgments

This work has been supported in part by NSF grant AST 0307252 and *Chandra* grant TM6-7004X (Smithsonian Astrophysical Observatory). ZM thanks COSPAR and the MPE for a travel grant to attend the Beijing meeting.

## References

Arons, J., Scharlemann, E.T. Pair formation above pulsar polar caps - Structure of the low altitude acceleration zone. *Astrophys. J.* 231, 854-879, 1979.

Beloborodov A.M., Thompson C. Corona of magnetars. *Astrophys. J.* (in press); e-print astro-ph/0602417.

Burwitz, V., Haberl, F., Neuhäuser, R., et al. The thermal radiation of the isolated neutron star RX J1856.5-3754 observed with Chandra and XMM-Newton. *Astron. Astrophys.* 399, 1109-1114, 2003.

Camilo, F., Ransom, S.M., Halpern, J.P., et al.. Transient pulsed radio emission from a magnetar. *Nature* 442, 892-895, 2006.

Cheng, A.F., Ruderman, M. Pair-production discharges above pulsar polar caps. *Astrophys. J.* 214, 598-606, 1977.

Gil, J., Melikidze, G.I., Geppert, U. Drifting subpulses and inner acceleration regions in radio pulsars. *Astron. Astrophys.* 407, 315-324, 2003.

Goldreich, P., Julian W.H.. Pulsar electrodynamics. *Astrophys. J.* 157, 869-880, 1969.

Harding, A.K., Muslimov, A.G. Particle acceleration zones above pulsar polar caps: Electron and positron pair formation fronts. *Astrophys. J.* 508, 328-346, 1998.

Ho, W.C.G., Kaplan, D.L., Chang, P., van Adelsberg, M., Potekhin, A.Y. Magnetic hydrogen atmosphere models and the neutron star RX J1856.5-3754. *Mon. Not. Roy. Astron. Soc.* (in press); e-print astro-ph/0612145.

Jones, P.B. Density functional calculations of the ground-state energies of atoms and infinite linear molecules in very strong magnetic fields. *Mon. Not. Roy. Astron. Soc.* 216, 503-510, 1985.

Jones, P.B. Properties of condensed matter in very strong magnetic fields. *Mon. Not. Roy. Astron. Soc.* 218, 477-485, 1986.

Kaspi, V.M., Gavriil, F.P. (Anomalous) X-ray pulsars. *Nuc. Phys. B Proc. Suppl.*, 132, 456-465, 2004.

Kaspi, V.M., McLaughlin, M.A. Chandra x-ray detection of the high magnetic field radio pulsar PSR J1718-3718. *Astrophys. J.* 618, 41-44, 2005.

Lai, D. Matter in strong magnetic fields. *Rev. Mod. Phys.* 73, 629-661, 2001.

Lai, D., Salpeter, E.E. Hydrogen Phases on the Surface of a Strongly Magnetized Neutron Star. *Astrophys. J.* 491, 270-285, 1997.

Medin, Z., Lai, D. Density-functional-theory calculations of matter in strong

magnetic fields. I. Atoms and molecules. *Phys. Rev. A* 74, 062507-1-14, 2006 [ML06a].

Medin, Z., Lai, D. Density-functional-theory calculations of matter in strong magnetic fields. II. Infinite chains and condensed matter. *Phys. Rev. A* 74, 062508-1-20, 2006 [ML06b].

Mori, K., Ruderman, M. Isolated magnetar spin-down, soft x-ray emission, and RX J1856.5-37542003. *Astrophys. J.* 592, L75-L78, 2003.

Neuhauser, D., Koonin, S.E., Langanke, K. Structure of matter in strong magnetic fields. *Phys. Rev. A* 36, 4163-4175, 1987.

Pérez-Azorín, J.F., Miralles, J.A., Pons, J.A. Anisotropic thermal emission from magnetized neutron stars. *Astron. Astrophys.* 451, 1009-1024, 2006.

Ruder, H., Wunner, G., Herold, H., Geyer, F. Atoms in Strong Magnetic Fields. Springer-Verlag, Berlin, 1994.

Ruderman, M. Matter in superstrong magnetic fields, in: Hansen, C.J (Ed.), Physics of Dense Matter. Proc. IAU Symp. 53, Reidel, Dordrecht-Holland/Boston, pp. 117-131, 1974.

Ruderman, M., Sutherland, P.G. Theory of pulsars - Polar caps, sparks, and coherent microwave radiation. *Astrophys. J.* 196, 51-72, 1975.

Tsong, T. T. Atom-probe field ion microscopy: Field ion emission and surfaces and interfaces at atomic resolution. Cambridge University, Cambridge, 1990.

Turolla, R., Zane, S., Drake, J.J. Bare quark stars or naked neutron stars? The case of RX J1856.5-37542004. *Astrophys. J.* 603, 265-282, 2004.

Usov, V.V., Melrose, D.B. Bound pair creation in polar gaps and gamma-ray emission from radio pulsars. *Astrophys. J.* 464, 306-315, 1996.

van Adelsberg, M., Lai, D., Potekhin, A.Y., Arras, P. Radiation from condensed surface of magnetic neutron stars. *Astrophys. J.* 628, 902-913, 2005.

van Kerkwijk, M.H., Kaplan, D.L. Isolated neutron stars: Magnetic fields, distances, and spectra, to appear in: Page, D., Turolla, R. Zane, S. (Eds.), Isolated neutron stars: from the interior to the surface. Proc. Astrophys. and Space Sci.; e-print astro-ph/0607277.

Woods, P.M., Thompson, C. Soft gamma repeaters and anomalous x-ray pulsars: Magnetar candidates, to appear in: Lewin, W.H.G., van der Klis, M. (Eds.), Compact stellar x-ray sources. Cambridge University, Cambridge; e-print astro-ph/0406133.